ELSEVIER

Characterisation of microstructural and sound absorption properties of porous asphalt subjected to progressive clogging

Mohd Zul Hanif Mahmud [a], Norhidayah Abdul Hassan [a,*], Mohd Rosli Hainin [a,b], Che Ros Ismail [a], Ramadhansyah Putra Jaya [b], Muhammad Naqiuddin Mohd Warid [a], Haryati Yaacob [a], Nordiana Mashros [a]

[a] School of Civil Engineering, Faculty of Engineering, Universiti Teknologi Malaysia, 81310 UTM Skudai, Johor, Malaysia
[b] Department of Civil Engineering, College of Engineering, Universiti Malaysia Pahang, 26300 Gambang, Pahang, Malaysia

HIGHLIGHTS

- A research framework to conduct progressive clogging conditions.
- A research framework to analyse microstructural properties of clogged porous asphalt.
- Recommend using Non-Local Mean filter in analysing clogged porous asphalt images.
- Severe clogging changed the air void structure and properties of porous asphalt.
- Low frequency sound wave energy can penetrate deeper into dense clogged surface.

ARTICLE INFO

ABSTRACT

Road traffic noise is a significant environmental issue. Porous asphalt is often used to mitigate this problem. However, the clogging issue is one of the main challenges of using porous asphalt. Clogging leads to a significant reduction in permeability and sound absorption as the pavement aged. This study measures the changes in the microstructural properties and sound absorption with multiple clogging cycles via X-ray Computed Tomography scanning. The identification of the presence of clogging particles in the X-ray images is also one of the challenges due to the complexity of image segmentation. Clogging simulation tests are performed on the compacted samples at a concentration of 1.0 g/l and repeated for five clogging cycles. The microstructural analysis shows that severe clogging densification occurred at the top section of the porous asphalt (approximately one-third of the sample height), thereby leading to alteration in the physical void structure and void properties (i.e., percentage, number, and size). Accordingly, the peak of the sound absorption coefficient observed at 800 Hz under an initial condition shifted to a new peak of 630 Hz after severe clogging. Low-frequency sound wave energy has a low attenuation energy that can penetrate the clogged surface given the correlation between the sound absorption coefficient and the air void properties. This study also recommends the use of Non-local mean filter to minimise the effect of white noise (equal signal intensity or density) and improve the accuracy of image segmentation.

1. Introduction

Porous asphalt was initially introduced in the United Kingdom (UK) in the early 1960 s, and its mixture design was developed by the Transport Research Laboratory [1]. Porous asphalt was initially used on military airfield airport runways and later applied on public roads. Porous asphalt was introduced on highways to reduce hydroplaning and spray particularly on heavy rain conditions. After a few trials in UK, a study reported that porous asphalt also provides acoustic benefits to road users and later was categorised as a type of low-noise road surface [1]. Chu et al. (2017) reported that traffic noise is the main cause in noise pollution, particularly in urban areas [2]. A study discovered that high exposure to traffic noise affects the surrounding community, particularly sleep disturbance and other health risks, such as fatigue, hypertension, and mental health [3–5]. Porous asphalt is effective in

* Corresponding author.
E-mail addresses: mzhanif@utm.my (M.Z.H. Mahmud), hnorhidayah@utm.my (N.A. Hassan), roslihainin@ump.edu.my (M.R. Hainin), cheros@utm.my (C.R. Ismail), ramadhansyah@ump.edu.my (R.P. Jaya), naqiuddin@utm.my (M.N.M. Warid), haryatiyaacob@utm.my (H. Yaacob), mnordiana@utm.my (N. Mashros).

Mohd Zul Hanif Mahmud, Norhidayah Abdul Hassan, Mohd Rosli Hainin et al.

Construction and Building Materials 283 (2021) 122654

controlling noise pollution from moving vehicles at a medium or high speed [6–7]. Numerous researchers have also found that porous asphalt can reduce approximately 2 dB(A) to 5 dB(A) compared with the conventional dense graded asphalt mixture [8–11]. The porous internal structure enables the asphalt to absorb sound wave energy and convert it into a low-grade heat [12–14]. Thus, less sound wave energy was reflected from the pavement surface into the surrounding.

However, clogging is the main issue in the use of porous asphalt. Porous asphalt is applied because the pavement needs to maintain its functional performance, particularly in reducing traffic noise throughout the pavement service life [9–11,15–16]. The ability of the porous asphalt to absorb traffic noise gradually depletes and eventually generates the same level of noise with a dense grade asphalt mixture as the pavement aged (2 or 3 years) [9–10,17]. Chen et al. (2013) measured the noise level at the travelling speed of 90 km/h and found that the sound intensity levels of porous asphalt increased to approximately 5 dB(A) over the period of 4 years as the pavement aged [9]. Takahashi (2013) and Yu et al. (2014) also obtained similar findings in the increase of sound level intensity on the basis of long-term field monitoring of porous asphalt [10,17]. Chen et al. (2013) also found that the noise levels of porous asphalt increased by approximately 1 dB(A) with the decrease of the air void content of porous asphalt by 1% [9]. Numerous researchers have also identified that the cause of the increment in the sound level intensity was due to the effect of clogging and densification of porous asphalt [9–10,17]. Clogging particles, such as dirt and debris, fill the void structure of the porous asphalt after few years of service and partially loss the benefits of sound absorption and permeability. Another source of clogging in porous asphalt is due to binder creep which occurs due to gravitational force which disrupt the voids interconnectivity of porous asphalt over extended period of time [18]. This phenomenon clearly shows that the changes in the air void structure, namely, distribution, percentage, number, and size, have significant effects on the functional performance of porous asphalt [9,19–22].

Fortunately, with the improvement in imaging technology i.e. X-ray Computed Tomography (CT) scanner, the machine can capture and monitor the microstructural properties of porous asphalt as the samples were progressively clogged. X-ray CT scanning is a non-destructive imaging technique that captures the X-ray images from different angles to generate multiple image cross-sections [23–25]. However, the identification of the clogging particles, particularly for repeated image scanning, is the main challenge in analysing the clogged porous asphalt images. This issue is due to the small difference in densities between the aggregate and the clogging particles that reflects the grey levels captured by an X-ray CT scanner. Therefore, this study characterised the effect of clogging on the basis of the changes that occurs within the void structure and void properties as the samples were progressively clogged.

This study aims to improve the understanding on the effect of progressive clogging towards the air void properties and sound absorption characteristics of porous asphalt. Moreover, this study developed a clogging simulation method that considers the effect of repeated clogging cycles on the microstructural properties and the acoustic performance. An imaging procedure is also proposed to monitor the changes of void properties, such as distribution, percentage, number, and size, subjected to progressive clogging.

2. Material and methods

2.1. Materials and sample preparation

The porous asphalt samples were laboratory fabricated in accordance with the Malaysian Public Works Department for road work specification [26]. The samples were prepared using granite aggregate and sieved to fit the Australian porous asphalt enveloped (Fig. 1) of 13.2 mm nominal maximum aggregate size [27]. This study used Performance Graded 76 (PG 76) as the binder at the designed bitumen content of 5.25%. Hydrated lime was used as an antistripping agent. The materials were mixed and compacted at 190 °C and 170 °C, respectively. The samples were compacted with a gyratory compactor at 50 gyrations to obtain the desired dimension at 50 mm (thickness) × 100 mm (diameter) at the estimated air void content of 20%. The detailed material properties of the samples are shown in Table 1.

The clogging material was collected with a handheld vacuum cleaner at the Skudai-Pontian highway, Federal Route 5, Johor, Malaysia to simulate the clogging cycles (Fig. 2a). The clogging materials consisted of dust, debris and fine aggregate particles. The site has high water runoff and traffic volume. Fig. 2b shows the image of the clogging particles (angular grain structure) captured with a Field Emission Scanning Electron Microscope (FESEM). The clogging material was then dry sieved (Table 2). The sieve analysis shows that the clogging material mostly consists of a coarse sandy material with less than 10% fine particles passing a 75 μm sieve size. The specific gravity of the clogging materials is 2.583. This factor was determined with a gas pycnometer according to ASTM D5550 [28].

2.2. Laboratory clogging simulation

This study developed a laboratory scale procedure to simulate a progressive clogging environment of the porous asphalt sample by using a constant head permeameter (Fig. 3a and 3b). An aqueous solution (tap water) was mixed with the aforementioned clogging material at the concentration of 1.0 g/l. The solution was magnetically stirred for 5 min at a constant revolution of 800 rpm. The laboratory clogging simulation was performed at ambient temperature for five clogging cycles. The detailed procedure of the clogging process is summarised as follows:

1. A virgin sample of porous asphalt (Fig. 3c) was placed into the constant head permeameter, and tap water was applied for approximately 5 min.
2. A constant head permeability test was then performed on a virgin sample for 30 s, and the volume of water discharged was measured.
3. The clogging solution was poured into the permeameter tube.
4. Fresh tap water was applied into the permeameter tube for approximately 5 min before a permeability test was performed.
5. A constant head permeability test was conducted on the sample, and the volume of water was measured for 30 s.
6. After the permeability test was completed, the sample was oven dried for 24 h for hardening.
7. The clogged sample (Fig. 3d) was then scanned with an X-ray CT scanner, followed by an impedance tube test.
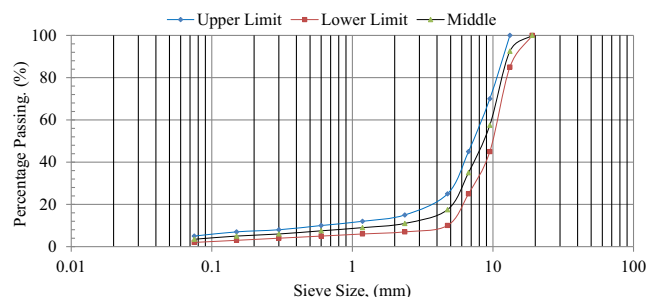

Fig. 1. Australian porous asphalt gradation [27].

Mohd Zul Hanif Mahmud, Norhidayah Abdul Hassan, Mohd Rosli Hainin et al.

Construction and Building Materials 283 (2021) 122654

Table 1
Aggregate and Binder Properties [25]

Materials	Physical Properties	
Coarse Aggregate	Bulk Specific Gravity	2.601
	Water Absorption	0.9%
	Aggregate Impact Value	26.0%
Fine Aggregate	Bulk Specific Gravity	2.427
	Water Absorption	2.0%
PG 76	Specific gravity at 25 °C	1.030
	Penetration Test at 25 °C	44 PEN
	Viscosity at 135 °C	1.04 Pa·s
	Viscosity at 165 °C	0.40 Pa·s
	G*/Sin δ, kPa at 76 °C	1.6 kPa

8. Steps 3 to 7 were repeated for additional four clogging cycles.

2.3. Microstructural investigation

The microstructural properties of the porous asphalt sample subjected to progressive clogging were monitored on the basis of the changes in the air void properties. Understanding this effect is significant since the air void characteristics (i.e. distributions, percentage, size and number) affect the sound absorption [2,9,19,22,29]. The changes of the air void properties with the presence of clogging particles should be measured using the image analysis technique. In this study, the investigation in the microstructure of porous asphalt was conducted with an X-ray CT scanner. The X-ray CT images were processed and analysed using two types of imaging software, namely, ImageJ and Avizo. The digital image processing that considers the presence of clogging particles was performed as in Mahmud et al. (2017) (Fig. 4) [25]. The image processing procedure is divided into two main stages. The first stage focuses on basic image processing on raw images obtained from the X-ray CT scanner by using ImageJ software (i.e. stack images, image conversion, cropping and scaling). The second stage of the microstructural investigation in Fig. 4 focuses on monitoring the changes in the air void properties of porous asphalt that was subjected to progressive clogging cycles. In this stage, the images were filtered with a Non-local means algorithm by using Avizo software. Data obtained from the image enhancement process was extracted using ImageJ software to obtain the image histogram of the selected air void area. This data was cumulatively summed and later converted into percentage of air voids. By using ImageJ, the images were then thresholded to void percentage and verified with the air void content determined in accordance with ASTM D3203 [30]. In addition, the air void

properties such as void size and number were also analysed using ImageJ, and the changes in the void properties were monitored for each clogging cycle.

2.3.1. X-ray CT scanner

In this study, the microstructural investigation is performed with an X-ray CT scanner (Fig. 5a) to acquire the internal structure of the porous asphalt cross-sectional view. The X-ray CT scanner (inspeXio smx-225 CT) with a maximum output voltage of 225 kV uses a cone beam method to reconstruct the internal structure of porous asphalt. In this study, the X-ray CT scanner is set at 190 kV as the output voltage and the ampere at 100 μA. The scanning starts from the source of X-ray energy penetrating through the sample as it rotates for 360 °C (Fig. 3b). The difference in X-ray energy as it penetrates through the sample is collected by the detector. The sample was scanned at 0.1 mm interval from the top to bottom of the sample. The scanning captures 1200 views at each angle of rotation with an average count of 15 times. The increase in the number of view and counts can improve the image accuracy but will lead to a long scan duration. The multiple cross-sectional images captured from the scanning are then combined from top to bottom as a stack at the interval of 0.1 mm (Fig. 5c). The image resolution from the combined stack images is 0.106 mm/pixel.

2.3.2. Digital image processing

Raw images obtained from the X-ray CT scanner were converted from 16 bits to 8 bits image by using ImageJ software. The 8 bit image consisted of 256 grey values, that is, 0 exhibits black colour (low density element, i.e. air voids) and 255 exhibits white colour (high density element, i.e. coated aggregate or clogging particles). In this study, a few image slices located at the top and bottom of the sample were removed due to image distortion that occurred during the scanning. The images were then cropped and scaled to the actual dimension of the compacted sample. The images obtained from X-ray CT scanning are seldom in perfect conditions (Fig. 6a), and they demonstrate poor contrast, disproportional illumination and excessive noise [24–25,31]. The image requires image treatment, which uses mathematical algorithms, such as contrast enhancement and image filter (nonlocal mean algorithm) (Fig. 6b). The Non-local mean filter algorithm was applied on the images by using Avizo imaging software to denoise image in a scalar volume. This mechanism is more effective particularly in a set of images that consist of white noise (equal signal intensity or density) compared with a conventional image filter (i.e. Gaussian filter) (Fig. 7). Such technique can preserve the existing properties

(a)   (b)

Fig. 2. Images of clogging materials (a) raw sample and (b) FESEM image.

Table 2
Dry sieve for clogging materials.

| Sieve Size (mm)	Cumulative Percentage Passing (%)
2.36	100.0
1.18	94.5
0.6	80.0
0.425	63.0
0.3	42.6
0.15	13.5
0.075	2.1

in the images, even the small features during filtering. This feature is important when highlighting the small difference in a specific gravity between the coated aggregate and the clogging particles because it can reduce the error when selecting the appropriate section of interest during segmentation process (Fig. 6c). Once the

image thresholding process is completed, the image is converted into a binary image (Fig. 6d) for further analysis.

After the quality of the stack images was refined, the changes in the air void properties of porous asphalt as the sample was subjected to repeated clogging cycles from virgin to clog conditions were measured. The analysis on the air void properties, particularly on the air void interconnectivity, is significant because the presence of clogging particles will cause changes to the physical properties of the air voids (disturbed the air void interconnectivity), namely, the content, size and numbers. In the void analysis, the Maximum Feret's diameter was set as a parameter in ImageJ software to determine the changes in the size of air voids. In the void analysis, the Maximum Feret's (F_{max}) diameter was set as a parameter in ImageJ software to determine the changes in the size of air voids. The aforementioned parameter, F_{max} is referred to the maximum distance between two pixels of two air void's boundary as
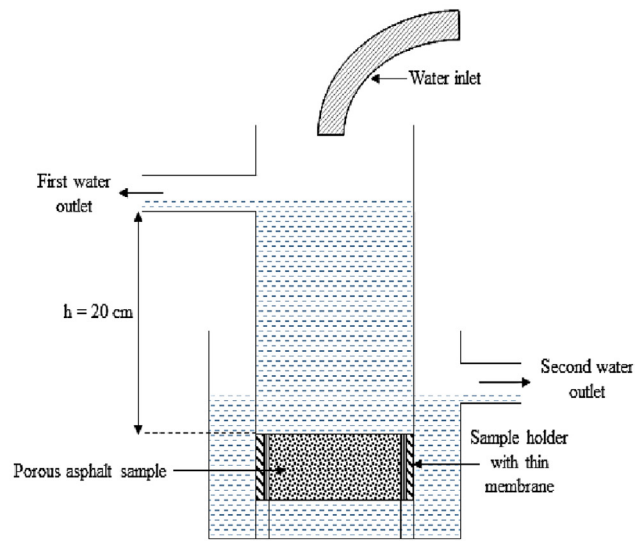
Fig. 3. Laboratory clogging simulation (a) constant head permeameter apparatus, (b) schematic constant head permeameter, (c) porous asphalt sample, and (d) clogged sample.
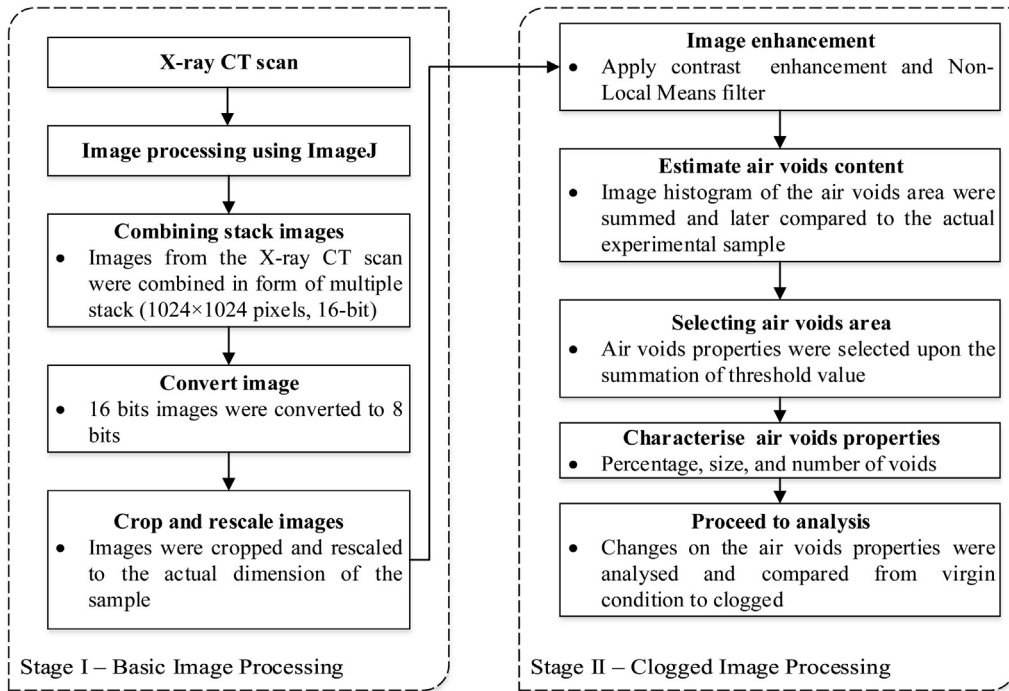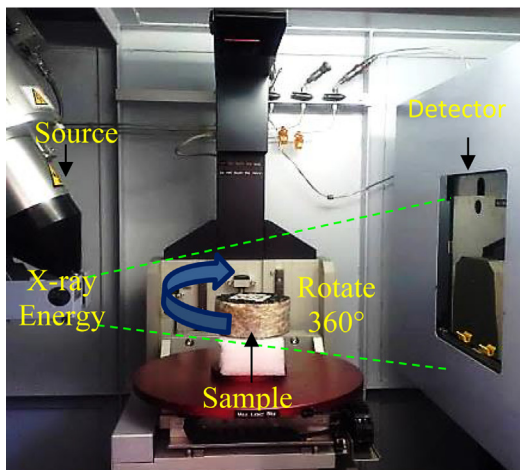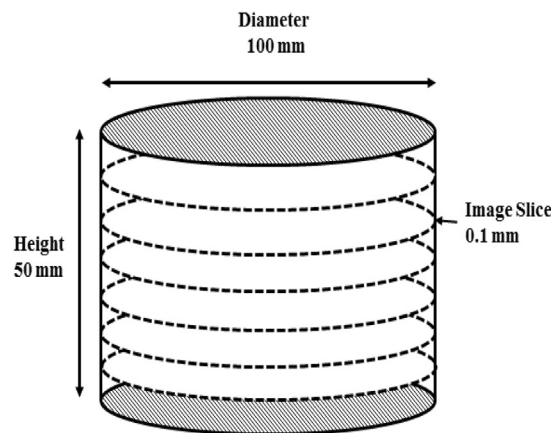
Fig. 4. Digital image processing procedure for clogged porous asphalt.

(a)

Fig. 5. Microstructure investigation (a) X-ray CT scanner, (b) X-ray CT chamber and (c) 2D stack images.

Mohd Zul Hanif Mahmud, Norhidayah Abdul Hassan, Mohd Rosli Hainin et al.

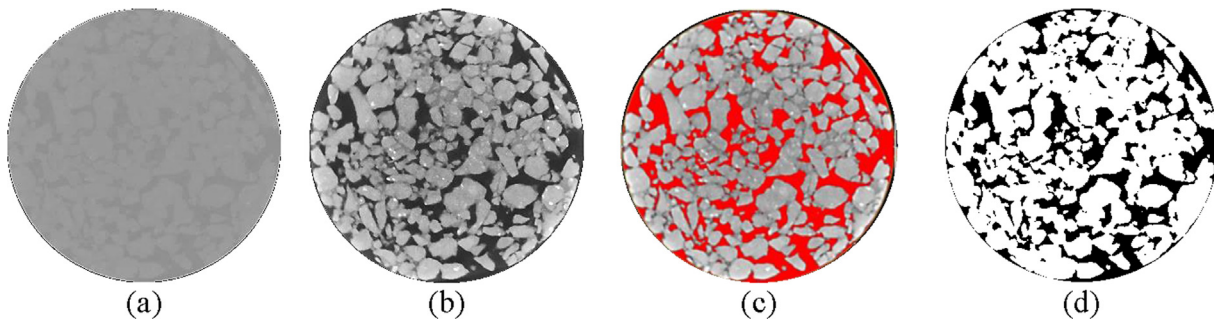Construction and Building Materials 283 (2021) 122654

Fig. 6. Digital image processing (a) raw image, (b) contrast adjustment and filtered, (c) image thresholding, and (d) binary image.
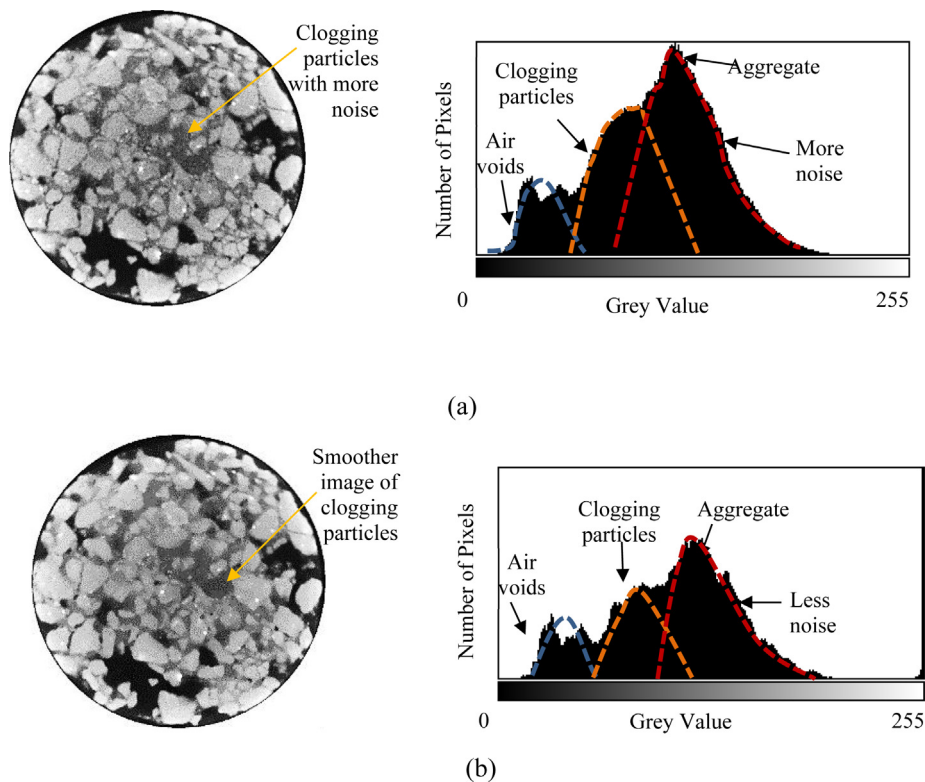

Fig. 7. Image comparison between (a) Gaussian filter and (b) Non-local means filter.

illustrated in Fig. 8. This parameter was mainly used because the air voids in the porous asphalt exhibit a predominantly elongated shape rather than a circular one due to the void connectivity, as reported by Mahmud et al. (2017) [25]. The changes on the number and air void content of porous asphalt were also analysed using ImageJ.

2.4. Sound absorption investigation

In this study, the measurement of sound absorption of porous asphalt was conducted using an impedance tube test that uses two microphones and a digital frequency analytical system (Fig. 9a). The impedance tube test (model – SCS 9020B/K) (Fig. 9b) was performed in accordance with the ASTM E1050 specification [32]. This method is effective in measuring the relative value of sound absorption at different ranges of frequency in a form of sound absorption coefficient (α) (Equation (1)). The sound absorption coefficient (α) reflects the ability of the material to absorb, reflect and dissipate the sound energy. This equipment
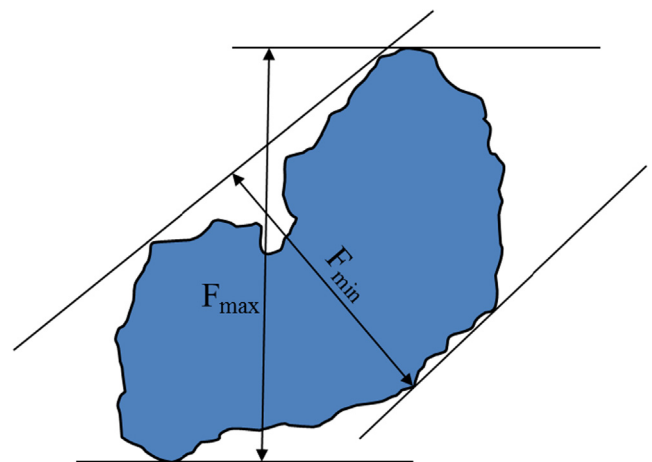

Fig. 8. Feret's diameter (F_{max}) of a selection region [24].

Mohd Zul Hanif Mahmud, Norhidayah Abdul Hassan, Mohd Rosli Hainin et al.

Construction and Building Materials 283 (2021) 122654
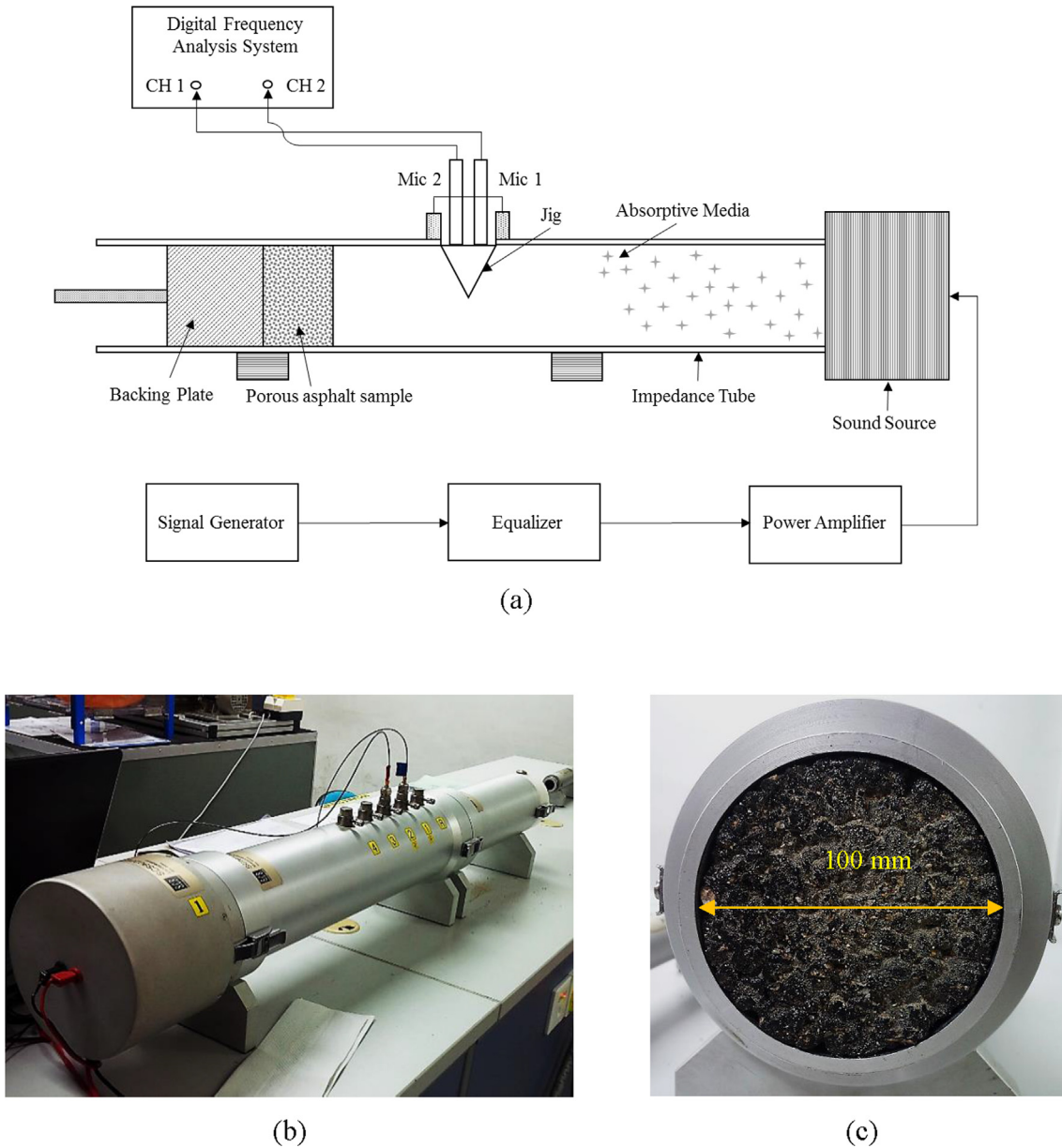
(a)

(b)　　　　　　　　　　　　　　　　　　(c)

Fig. 9. Impedance tube test (a) schematic diagram, (b) impedance tube equipment, and (c) porous asphalt sample.

can measure low and high frequency sound wave covering from 100 Hz to 5000 Hz. A large tube with a diameter of 100 mm is used for a low range frequency (Fig. 9c). Meanwhile, a small tube with a diameter of 28 mm is used for a high range frequency. In this study, the measurement of sound absorption coefficient for low range frequency is limited from 200 Hz to 1600 Hz. This step is conducted because the noise generated due to the interaction between tyre and pavement from moving vehicles is mostly substantial to human ears at a range of 800 Hz to 1200 Hz [1,33]. The study on the effect of clogging on the sound absorption of porous asphalt that uses a low range frequency is already sufficient to measure the changes caused by the clogging particles. Ten one-third octave bandwidth frequencies (i.e. 200, 250, 315, 400, 500, 630, 800, 1000, 1250 and 1600 Hz) were used as fixed ranges of bandwidth frequency. The impedance tube test was performed in dry condition for every clogging cycle from virgin to clog conditions. The test was conducted at the temperature of 25 °C with a relative humidity of 60%.

$$\alpha = 1 - \frac{I_r}{I_i} \tag{1}$$

where:
α = Sound absorption coefficient,
I_r = Reflected sound intensity, and
I_i = Incident sound intensity.

3. Result and discussion

3.1. Effect of clogging on air void

3.1.1. Air void distribution

The result of void distribution from the top (0 height ratio) to the bottom (1 height ratio) section of the sample for five repeated clogging cycles is shown in Fig. 10. The figure shows that the air void is homogeneously distributed throughout the sample at cycle 0 (initial/virgin condition). A transition trend was observed as the

Mohd Zul Hanif Mahmud, Norhidayah Abdul Hassan, Mohd Rosli Hainin et al.

Construction and Building Materials 283 (2021) 122654

sample was repeatedly clogged. The gradual reduction of the air void content for each clogging cycle, particularly at the top section (height ratio of 0 to 0.3), varied from 1% to 2%. The densification effect of the clogging particles is one of the main reasons of this transition. The surface of porous asphalt consists of a high surface area with a large and connected air void structure. This situation has caused the clogging particles to permeate into the porous asphalt and later sediment inside the air void channel. The severe sedimentation of clogging particles will prevent the movement of other clogging particle from flowing out of the internal structure of the porous asphalt. This effect can clearly be seen in Fig. 10 where minor changes to the air void content are observed from the height ratio of 0.3 to 1.0. In summary, the effect of clogging shows severe changes towards the air void content of porous asphalt at one-third of the top section of the sample height with a clear transition pattern as the sample was repeatedly clogged.

3.1.2. Air void properties

The air void properties were characterised in terms of air void content, size and number. Fig. 10 shows that the distribution of the air void content throughout the sample is mostly affected at one-third of the top section due to the densification of the clogging particles. The effect of clogging densification can also be identified by overlapping the images (superimpose technique) initially captured and after the 5th cycle using the ImageJ software (Fig. 11). The superimpose process merges two set of colour channels of the images. In this study, the initial set of images is set to be in red colour while the second set is in yellow colour. The overlapped colour (green) gives the indication of new element (clogged regions) developed due to progressive clogging. In order to ensure the accuracy of the superimpose images and data interpretation, the captured images were consistently cropped to its initial dimension and analysed in a combined stack at a very small interval of 0.1 mm and high resolution of 0.106 mm/pixel. The stack of the images was virtually cut and equally divided into three main sections, namely, top, middle and bottom for better interpretation of the clogging material distribution throughout the sample. To further verify the accuracy of the superimpose, the materials phases (voids, aggregate and mastic) of the cut sections were comparably analysed for their composition. The image clearly supports that the concentration of the clogging material mainly occurs at the top section of the sample.

Fig. 12 shows the result of the air void properties, namely, air void content, number and size, that were affected by the progressive clogging condition determined for the top, middle and bottom sections. Under virgin condition, the air void content in Fig. 12 shows a comparable high air void content at the top and bottom sections of the sample. Meanwhile, a low air void content is measured at the middle section. The high air void content at the top and bottom sections of the compacted sample may be due to the confinement effect that occurred during compaction. At the middle
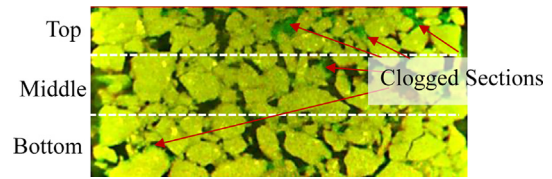

Fig. 11. Overlapped coloured X-ray images (virtual cut section) of clogged sections for Cycle 0 and 5.

section, the aggregate particles were intensively compacted, and the air void content within this section was reduced. The bottom section of the sample has a larger mean air void size of approximately 1.5 mm than the top and bottom sections. This result is because of the 'gravitational effect' during mixing where large aggregate particles fall to the bottom of the mould, followed by the fines. Such phenomenon leads to a large air void size at the bottom of the sample.

The air void content at the top section was gradually reduced from 20.5% (cycle 0) to 16.6% (cycle 5) as the sample was repeatedly clogged from cycles 1 to 5. This value is an average of approximately 0.8% reduction for every clogging cycle. The results in Fig. 12b and 12c also show a significant reduction at the top section of the sample in terms of the number and size of the air voids as detected from the imaging software. The presence of clogging par-
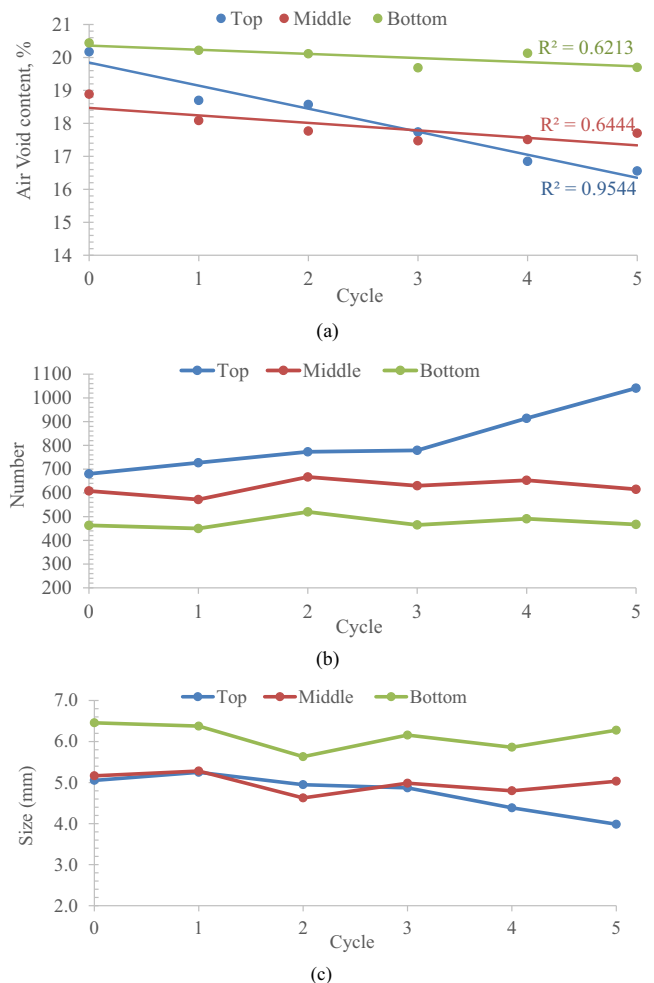

(a)

(b)

(c)

Fig. 12. Effect of clogging towards the air voids properties (a) air void content, (b) void number, and (c) void size.
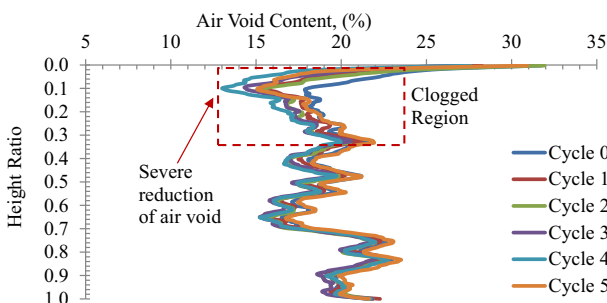

Fig. 10. Effect of repeated clogging cycle on the distributions of air void content.

ticles fills the existing voids structure and separates the air void particles. This phenomenon shows that the number of air void increases with the decrease in the size of air voids, thus reducing the air void interconnectivity. The middle and bottom sections of the sample experience minor changes towards the air void content, number and size. The physical properties of the clogging particles (sandy) also contribute to the outcome of small changes that occurred at the middle and bottom sections of the sample. The progressive build-up sedimentation (densification) of the clogging materials at the top section of the sample limits the movement of the clogging particles to be distributed to the middle and bottom sections of the sample. Accordingly, small changes towards the existing properties of porous asphalt (i.e. air void content, number and size) were observed. The results in Fig. 12b and 12c show fluctuations in term of the number and size of the air void, particularly at cycles 2 and 3, as the sample was repeatedly clogged. The mobilisation of the clogging particles was one of the main reasons of the fluctuation as the sample was repeatedly clogged. Fine clogging particles can easily mobilise and disperse or relocate into other parts of the internal structure of porous asphalt. The mobilisation of clogging particles refers to the particles that 'hop on hop off' the air void channel. This phenomenon can be seen in Fig. 13, from the overlapped X-ray images captured at cycles 2 and 3. The figure shows the self-cleaning ability of porous asphalt at three different sections as a result of progressive clogging. A less mobilisation effect was observed at the top section due to the densification of clogging particles (Fig. 13a). However, this effect frequently occurs at the middle and bottom sections of the sample.

3.2. Effect of clogging on the sound absorption of porous asphalt

Fig. 14 shows the result of the sound absorption coefficient of porous asphalt that is measured at one-third octave bandwidth frequencies (i.e. 200, 250, 315, 400, 500, 630, 800, 1000, 1250 and 1600 Hz) as the sample was progressively clogged. The outcome of the impedance tube test is based upon the changes in the volumetric properties (air void content) of porous asphalt that is approximately from 20% to 16%. The effect of progressive clogging is generally insignificant at low (200 Hz) and high (1600 Hz) frequencies. The result shows only minor changes of the sound absorption coefficient ranging from 0.01 to 0.03 as the sample was progressively clogged.

In the initial condition (cycle 0), the peak of the sound absorption coefficient of porous asphalt can be observed at 800 Hz with a value of 0.81. This finding indicates that the porous asphalt sample
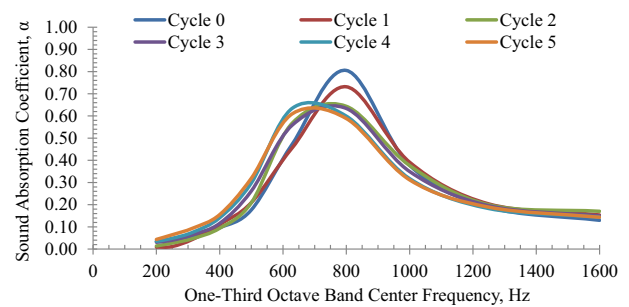

Fig. 14. Effect of clogging on sound absorption coefficient.

can absorb approximately 81% of the sound wave energy at 800 Hz without the effect of the clogging particles and reflect back 19% to the pavement surface (Fig. 15a). Previous research reported that the 800 Hz frequency also represents the typical tyre-road interaction of moving vehicles [12,34–36]. The major changes in the sound absorption coefficient occurred after the first clogging cycle, which causes a reduction from 0.81 (cycle 0) to 0.73 (cycle 1). This finding shows that approximately 27% of sound wave energy at 800 Hz is reflected to the pavement surface (Fig. 15b), which is 8% more sound wave energy without the clogging particles. The sound absorption increased due to the densification that occurs at the top section of the porous asphalt (Fig. 15b). This finding is also supported by the X-ray CT scanning result, which shows a significant reduction in the air void content at the top section of the sample after cycle 1 (Fig. 10). Kia et al. (2018) also found a similar observation and stated that clogging phenomenon starts as the clogging particles accumulate at the top surface of the pavement, thereby creating a dense layer [37]. The thickness of this layer increases as additional clogging cycles were applied. After densification, the peak of the sound coefficient significantly reduces with the clogging cycles until the fourth and fifth clogging cycles. Other changes occurred at the fourth and fifth cycles, and the recorded sound absorption coefficients were at 0.60 and 0.59, respectively. This change became insignificant due to severe densification (as illustrated in Fig. 15c), thereby leading to additional sound wave energy reflected back to the surface. Such change will reduce the efficiency of porous asphalt in mitigating the traffic noise that mainly occurred at 800 Hz as the pavement was clogged.

Detailed findings in Fig. 14 can be categorised into three main phases (Fig. 16). Phase one describes the changes in the sound absorption coefficient from cycles 0 to 1 because the results show
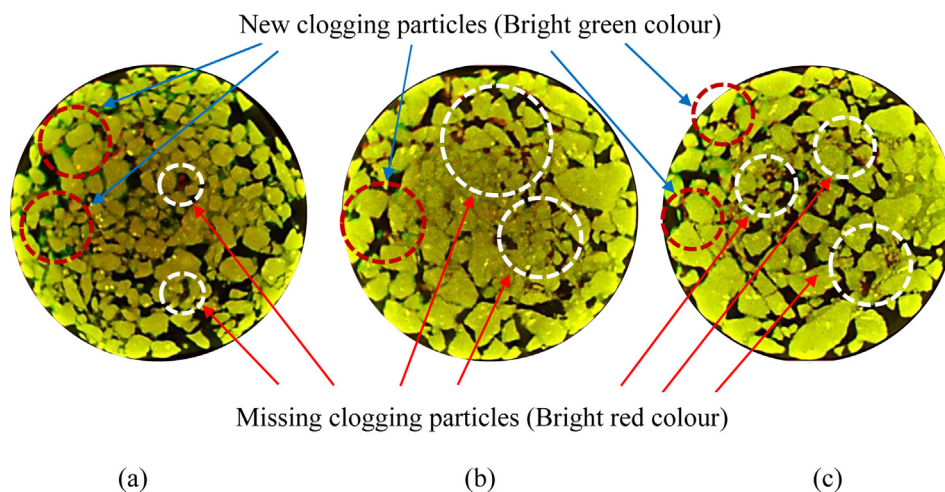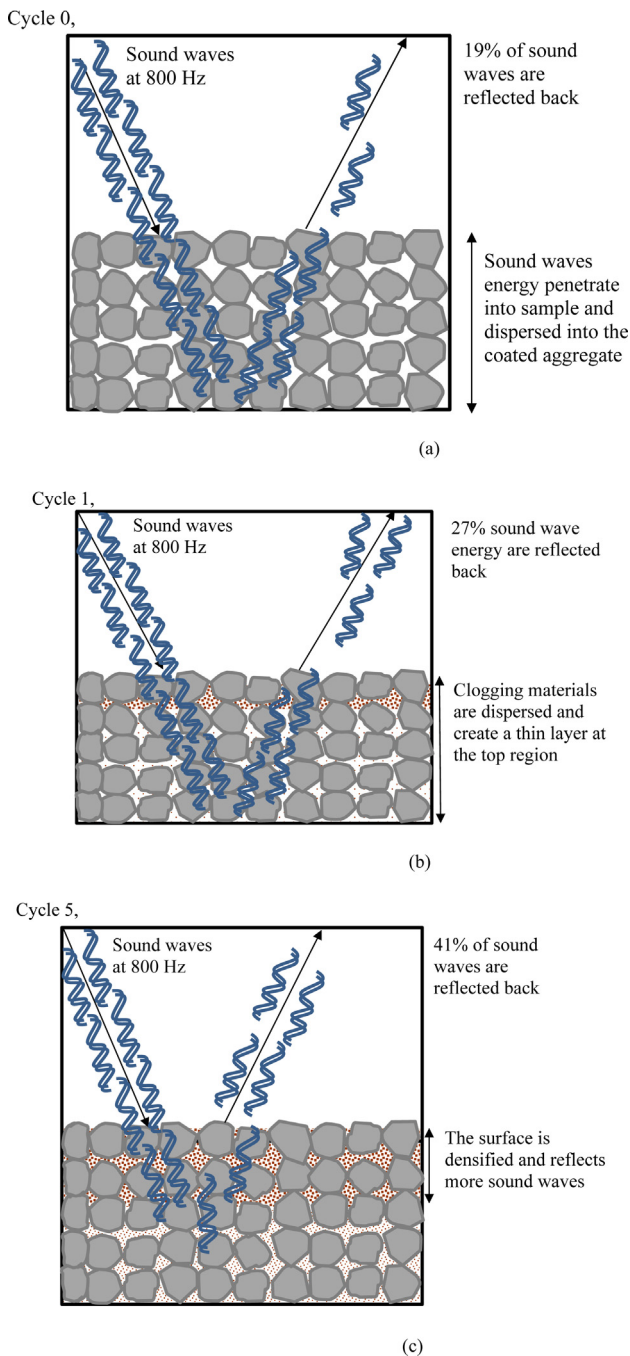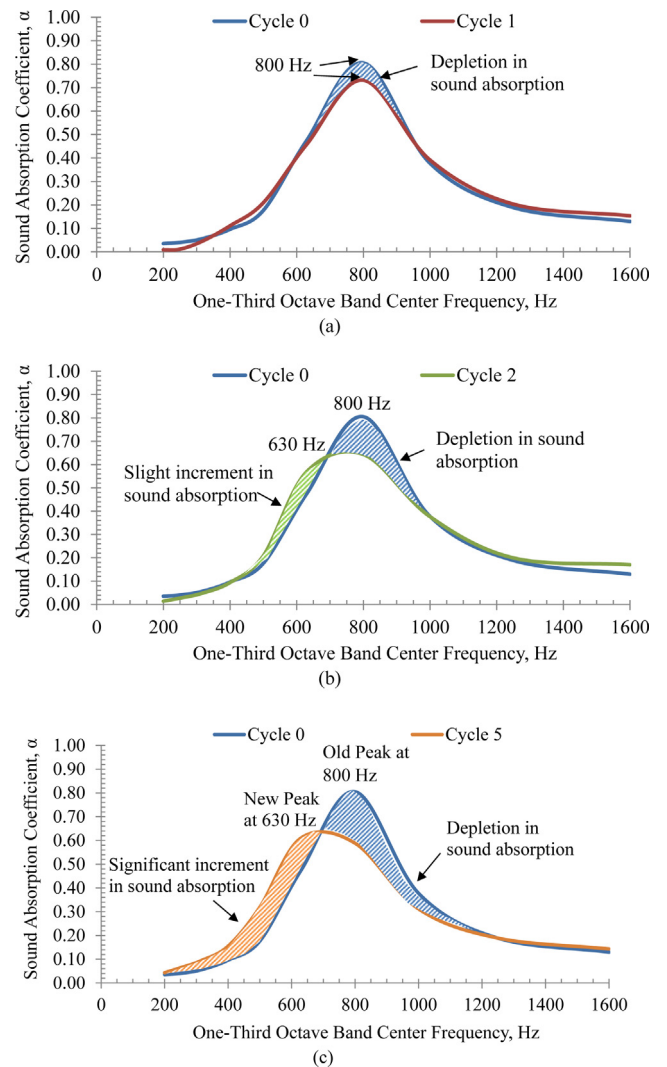

Fig. 13. Comparison of overlapped coloured X-ray images of Cycle 2 and 3 at (a) top, (b) middle and (c) bottom section.

Mohd Zul Hanif Mahmud, Norhidayah Abdul Hassan, Mohd Rosli Hainin et al.

Construction and Building Materials 283 (2021) 122654

Fig. 15. Illustrations of sound wave energy at 800 Hz passing through porous asphalt sample after (a) Cycle 0, (b) Cycle 1, and (c) Cycle 5.

Fig. 16. Comparison of the effect of clogging on sound absorption characteristics for (a) Phase 1, (b) Phase 2, and (c) Phase 3.

a significant reduction in the peak particularly at 800 Hz (Fig. 16a). This phenomenon is mainly due to the presence of clogging particles that tend to fill up the surface and internal structure of the porous asphalt. Fig. 16b compares the result of sound absorption coefficient at cycles 0 and 2, which reflects the second phase of the clogging behaviour. The curves show a slight increment at the mid-range frequency (450 Hz to 650 Hz) and significant reduction in coefficient at the frequency of 650 Hz to 100 Hz. At this stage, the clogging particles have densified the top section and changed the air void structure of the porous asphalt, thereby reducing the air void content and size and increasing the number of air void (Fig. 12). In phase three, further changes on the sound absorption coefficients have caused the pavement to absorb low

to mid-range sound wave frequency from 200 Hz to 650 Hz. Meanwhile, further reduction on the coefficients can be observed for the sound wave energy generated at 650 Hz to 1250 Hz. Fig. 16c shows that the peak of the sound absorption at 800 Hz has shifted to 630 Hz. As previously mentioned, clogging has changed the air void structure of the porous asphalt particularly at the top section. The sound energy had difficultly penetrating particularly at 650 Hz to 1250 Hz with the densification of the porous asphalt layer. This situation is because of the high frequency sound wave energy that has a higher rate of energy attenuation that makes it difficult to penetrate the sample compared with a lower range sound wave energy. Thus, this type of sound wave energy (approximately at 800 Hz to 1200 Hz) reflects to the surface and makes the surrounding environment louder.

3.3. Correlation between sound absorption coefficient and air void properties

As discussed in Section 3.1.1, the result of the microstructural investigation reveals a significant change towards the air void distribution due to progressive clogging. This situation had changed the air void structure particularly at the top section of the sample. Accordingly, the correlation is mainly focused on those aforementioned air void properties located at the top section and its effects

Mohd Zul Hanif Mahmud, Norhidayah Abdul Hassan, Mohd Rosli Hainin et al.

Construction and Building Materials 283 (2021) 122654

towards the sound absorption coefficient of porous asphalt. Fig. 16 shows that the peak of the sound absorption coefficient is at 800 Hz without the presence of clogging materials (cycle 0), which suitable to absorb traffic noise generated from moving vehicles. The peak significantly reduced and shifted to 630 Hz, particularly at the fifth clogging cycles, as the sample was progressively clogged. Figs. 17 and 18 correlate the sound absorption coefficient and air void properties (i.e. percentage, number and size) at 800 and 630 Hz, respectively.

Fig. 17 demonstrates that the result shows a positive correlation between the sound coefficient and the percentage and size of air void at 800 Hz frequency. This result indicates that porous asphalt is an effective medium in absorbing sound wave energy generated at 800 Hz with high air void content and large average void size at approximately 5 mm. By contrast, a negative correlation is observed with a void number, thereby showing that the sound absorption coefficient decreases because this phenomenon reduces the void connectivity within the sample (Fig. 17c). The presence of clogging particles creates a densified layer and increases the number of air voids as the accumulation of clogging particles splits the air voids into multiple fragments. Porous asphalt is a porous medium that converts sound wave energy (vibrating air void molecules) and slowly dissipates into heat energy as it passes through the porous structure [38]. The progressive clogging of the sample has densified the porous asphalt surface and caused changes towards the air void structure, thereby reducing the interconnected air voids with less percentage and size. Accordingly, the sound wave generated at
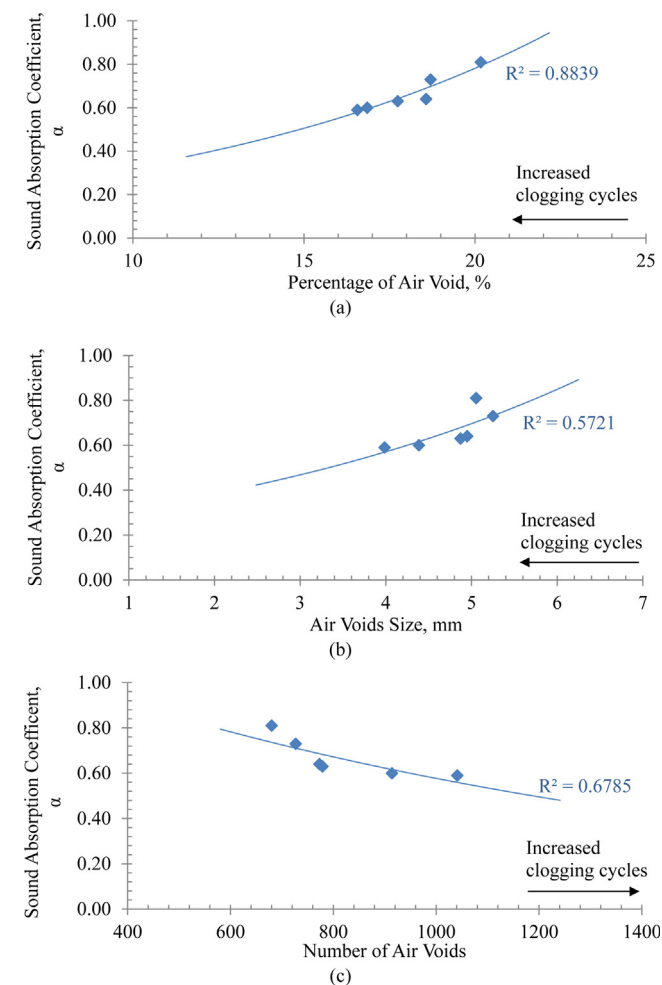

Fig. 17. Correlation of sound absorption coefficient at 800 Hz and air voids properties (a) percentage of air void, (b) size of air voids, and (c) number of voids.
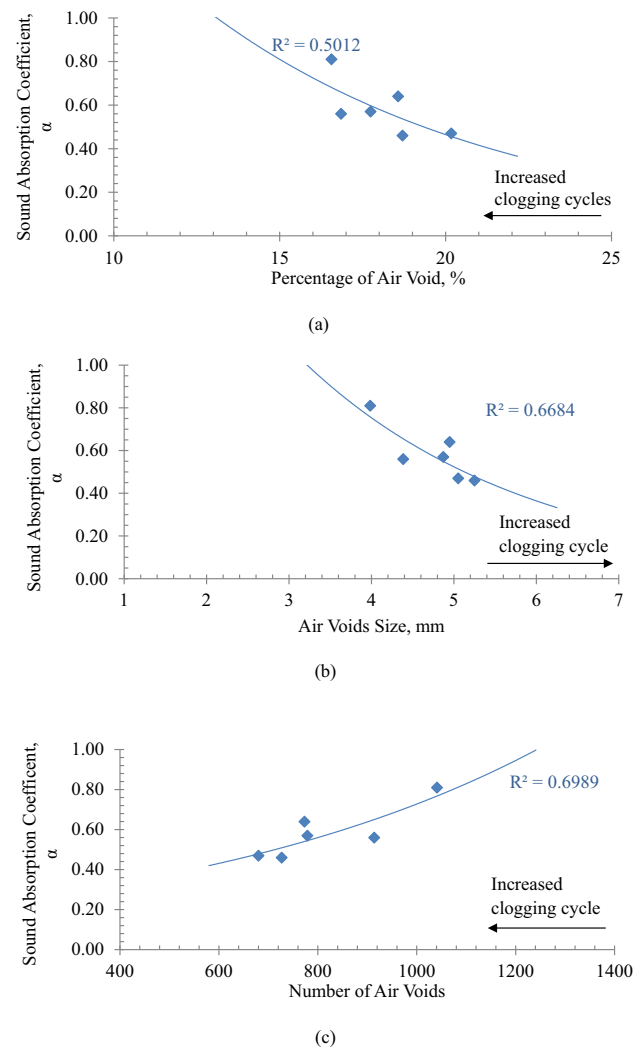

Fig. 18. Correlation of sound absorption coefficient at 630 Hz and air voids properties (a) percentage of air void, (b) air voids size, and (c) number of air voids.

800 Hz has difficulties penetrating into the clogged sample due to high attenuation. This situation led to additional sound wave reflected back to the surface. Consequently, the peak of the sound coefficient has shifted from 800 Hz to 630 Hz.

Fig. 18 shows the correlation between the sound absorption coefficients that occurred at 630 Hz and the air void properties. This finding seems to be in contrast with the result obtained at 800 Hz where the sound absorption increases with the void number. Sound wave energy generated at 630 Hz can penetrate deep into the densified layer of clogging particles in the porous asphalt. A shorter wavelength (high frequency) is more prone to be reflected, refracted and converted to heat energy compared with a longer wavelength (low frequency). A shorter wavelength can also deeply penetrate, thereby indicating that sound wave generated at 630 Hz has a superior penetration compared with 800 Hz (shallower penetration). This phenomenon is mainly contributed by the changes in the void structure and properties that experience a reduction in air void size and increment of void number. Accordingly, additional sound wave energy is absorbed at 630 Hz, and a new effective peak is established for sound absorption.

4. Conclusion

The following conclusions are summarised on the basis of the obtained results:

Mohd Zul Hanif Mahmud, Norhidayah Abdul Hassan, Mohd Rosli Hainin et al.

Construction and Building Materials 283 (2021) 122654

(a) The introduced laboratory clogging simulation procedure can apply a progressive clogging state within the internal structure of the porous asphalt to allow for clogging cycles to be conducted on the samples.

(b) A suitable image filtering algorithm should be applied to properly extract and analyse the X-ray CT images for accurate data interpretation. The digital imaging procedure highlights the importance of using Non-Local Mean filter to minimise the white noise due to equal signal intensity or material density.

(c) The progressive clogging phenomenon particularly from cycles 2 to 5 had caused significant changes towards the air void structure and properties. The top section (one-third of the sample height) was severely affected due to the accumulation of a densified layer of clogging particles as it progressively clogged. The percentage and size of the air void were significantly reduced with the increase in the number of voids.

(d) The changes in the microstructural properties of the porous asphalt have altered its capability to absorb sound wave energy at different frequencies. A densified clogging layer has reduced the sound absorption peak from 800 Hz to 630 Hz because a low sound wave energy provides less attenuation and can penetrate deep through the densified layers.

(e) The correlation between air void properties and sound absorption indicated that the high void content and large void size help improve sound absorption coefficient.

CRediT authorship contribution statement

Mohd Zul Hanif Mahmud: Writing - original draft. **Norhidayah Abdul Hassan**: Supervision. **Mohd Rosli Hainin**: Concpetualization. **Che Ros Ismail**: Data curation. **Ramadhansyah Putra Jaya**: Writing: review & editing. **Muhammad Naqiuddin Mohd Warid**: Methodology. **Haryati Yaacob:** Formal analysis. **Nordiana Mashros**: Writing, Visualization.

Declaration of Competing Interest

The authors declare that they have no known competing financial interests or personal relationships that could have appeared to influence the work reported in this paper.

Acknowledgments

References

[1] P. Morgan, Guidance manual for the implementation of low-noise road surfaces, FEHRL Report, Forum of European National Highway Research Laboratories, 2006.

[2] L. Chu, T.F. Fwa, K.H. Tan, Evaluation of wearing course mix designs on sound absorption improvement of porous asphalt pavement, Constr. Build. Mater. 141 (2017) 402–409.

[3] W. Babisch, W. Swart, D. Houthuijs, J. Selander, G. Bluhm, G. Pershagen, K. Dimakopoulou, A.S. Haralabidis, K. Katsouyanni, E. Davou, P. Sourtzi, E. Cadum, F. Vigna-Taglianti, S. Floud, P. Sourtzi, Exposure modifiers of the relationships of transportation noise with high blood pressure and noise annoyance, The J Acoust Soc Am 132 (6) (2012) 3788–3808.

[4] T. Beckenbauer, Road Traffic Noise. In Handbook of engineering acoustics, Springer, Berlin, Heidelberg, (2013), 367-392.

[5] T. Park, M. Kim, C. Jang, T. Choung, K. A. Sim, D. Seo, S. Chang, The Public Health Impact of Road-Traffic Noise in a Highly-Populated City, Republic of Korea: Annoyance and Sleep Disturbance. Sustainability, 10, (2018), 8, 2947.

[6] M. Li, Tyre-Road Noise, Surface Characteristics and Material Properties. (Doctoral dissertation), Delft University of Technology, Netherlands, 2013.

[7] A. Vaitkus, T. Andriejauskas, V. Vorobjovas, A. Jagniatinskis, B. Fiks, E. Zofka, Asphalt wearing course optimization for road traffic noise reduction, Constr. Build. Mater. 152 (2017) 345–356.

[8] P.S. Kandhal, Asphalt pavements mitigate tire/pavement noise, Hot Mix Asphalt Technology 9 (2) (2004) 22–31.

[9] J.S. Chen, W. Hsieh, M.C. Liao, Evaluation of functional properties of porous asphalt pavements subjected to clogging and densification of air voids, Transp. Res. Rec. 2369 (1) (2013). 68–76. S.

[10] S. Takahashi, Comprehensive study on the porous asphalt effects on expressways in Japan: based on field data analysis in the last decade, Road Mater. Pavement 14 (2) (2013) 239–255.

[11] M. Buret, J. McIntosh, C. Simpson, Long-term asphalt trial: Results of acoustic tests after three years, Acoust. Aust. 44 (2) (2016) 273–281.

[12] J.P. Arenas, M.J. Crocker, Recent trends in porous sound absorbing materials for noise control, J Sound. Vib. (2010) 12–17.

[13] H.S. Seddeq, Factors influencing acoustic performance of sound absorptive materials, Aust. J. Basic Appl. Sci. 3 (4) (2009) 4610–4617.

[14] L. Cao, Q. Fu, Y. Si, B. Ding, J. Yu, Porous materials for sound absorption, Compos. Commun. 10 (2018) 25–35.

[15] L.D. Poulikakos, M.N. Partl, A multi-scale fundamental investigation of moisture induced deterioration of porous asphalt concrete, Constr Build Mater 36 (2012) 1025–1035.

[16] L. Chu, T.F. Fwa, Functional sustainability of single-and double-layer porous asphalt pavements, Constr. Build. Mater. 197 (2019) 436–443.

[17] B. Yu, L. Jiao, F. Ni, J. Yang, Long-term field performance of porous asphalt pavement in China, Road Mater. Pavement 16 (1) (2014) 214–226.

[18] M.O. Hamzah, M.R.M. Hasan, M. van de Ven, Permeability loss in porous asphalt due to binder creep, Constr. Build. Mater. 30 (2012) 10–15.

[19] S. Alber, W. Ressel, P.F. Liu, D. Wang, M. Oeser, Influence of soiling phenomena on air-void microstructure and acoustic performance of porous asphalt pavement, Constr. Build. Mater. 158 (2018) 938–948.

[20] J. Hu, Z. Qian, P. Liu, D. Wang, M. Oeser, Investigation on the permeability of porous asphalt concrete based on microstructure analysis, Int. J. Pavement Eng. 1–11 (2019).

[21] M. Z. H. Mahmud, Functional performance and microstructural properties of porous asphalt subjected to clogging (Doctoral dissertation), Universiti Teknologi Malaysia, Malaysia, 2019.

[22] L. Gao, Z. Wang, J. Xie, Z. Wang, H. Li, Study on the sound absorption coefficient model for porous asphalt pavements based on a CT scanning technique, Constr. Build. Mater. 230 (2020) (2020).

[23] L. Tashman, E. Masad, B. Peterson, H. Saleh, Internal structure analysis of asphalt mixes to improve the simulation of Superpave gyratory compaction to field conditions, J. Assoc. Asphalt Paving Technol. 70 (2001) 605–645.

[24] N.A. Hassan, G.D. Airey, M.R. Hainin, Characterisation of micro-structural damage in asphalt mixtures using image analysis, Constr Build Mater 54 (2014) 27–38.

[25] M.Z.H. Mahmud, N.A. Hassan, M.R. Hainin, C.R. Ismail, Microstructural investigation on air void properties of porous asphalt using virtual cut section, Constr. Build. Mater. 155 (2017) 485–494.

[26] P.W.D. Malaysia, Standard Specification for Road Works, Section 4, Flexible Pavement, Jabatan Kerja Raya Malaysia, Kuala Lumpur, 2008.

[27] Australian Asphalt Pavement Association (AAPA), National Asphalt Specification, Australian Asphalt Association, 2004.

[28] ASTM D5550. Standard Test Method for Specific Gravity of Soil Solids by Gas Pycnometer. ASTM International, West Conshohocken, PA, 2014.

[29] F.G. Praticò, On the dependence of acoustic performance on pavement characteristics, Transport Res D-Tr E 29 (2014) 79–87.

[30] ASTM D 3203, Standard Test Method for Percent Air Voids in Compacted Dense and Open Bituminous Paving Mixtures, ASTM International, West Conshohocken, PA, 2011.

[31] N. A. Hassan, N. A. M. Abdullah, N. A. M. Shukry, M. Z. H. Mahmud, N. Z. M. Yunus, R. P. Jaya, M. R. Hainin, H. Yaacob, (2015). Laboratory evaluation on the effect of clogging on permeability of porous asphalt mixtures. J. Teknol., 76, (2015), 14, 77-84.

[32] ASTM E1050, Standard Test Method for Impedance and Absorption of Acoustical Materials Using a Tube, Two Microphones and a Digital Frequency Analysis System. ASTM International, West Conshohocken, PA, 2012.

[33] N. Neithalath, R. Garcia, J. Weiss, J. Olek, Tire-Pavement interaction noise: Recent research on concrete pavement surface type and texture, In Proceedings of the 8th International Conference on Concrete Pavements, (2005, August), Vol. 2, 523-540.

[34] U. Sandberg, Road traffic noise - The influence of the road surface and its characterization, Appl. Acoust. 21 (2) (1987) 97–118.

[35] J. Cesbrona, F. Anfosso-Ledee, D. Duhamel, H.P. Yin, D. Le Houedec, Experimental study of tyre/road contact forces in rolling conditions for noise prediction, J. Sound Vib. 320 (2009) 125–144.

[36] V.V. Saykin, Y. Zhang, Y. Cao, M.L. Wang, J.G. McDaniel, Pavement macrotexture monitoring through sound generated by a tire-pavement interaction, J. Eng. Mech. 139 (3) (2012) 264–271.

[37] A. Kia, H.S. Wong, H. S., C.R. Cheeseman, Defining clogging potential for permeable concrete, J. Environ. Manage. 220 (2018) 44–53.

[38] Y. Na, J. Lancaster, J. Casali, G. Cho, Sound absorption coefficients of micro-fiber fabrics by reverberation room method, Text. Res. J. 77 (5) (2007) 330–335.